Electronic Research Archive

http://www.aimspress.com/journal/era

ERA, 30(4): 1322–1339.
DOI: 10.3934/era.2022069
Received: 14 January 2022
Revised: 02 March 2022
Accepted: 13 March 2022
Published: 18 March 2022

*Research article*

# Dynamics in a predator-prey model with memory effect in predator and fear effect in prey

**Ruizhi Yang and Dan Jin***

Department of Mathematics, Northeast Forestry University, Harbin 150040, Heilongjiang, China

* **Correspondence:** Email: jindan720@163.com; Tel: +8615663526603.

**Abstract:** The spatial memory effect in predator and fear effect in prey are incorporated in a diffusive predator-prey model. We are interested in studying the dynamics generated by the memory effect and fear effect, and mainly study the local stability of coexisting equilibrium, the existence of Hopf bifurcation and the property of Hopf bifurcation. Through the numerical simulations, we show that increasing memory-based diffusion coefficient is not conducive to the stability of the coexisting equilibrium, and the fear effect has both stabilizing and destabilizing effect on the coexisting equilibrium under different parameters.

**Keywords:** predator-prey; delay; memory effect; fear effect; Hopf bifurcation

## 1. Introduction

The relationship between predator and prey is an important research content in ecosystem, and many scholars have studied this interaction by differential equation models [1–6]. The direct relationship between predator and prey is the consumption of prey. One of the indirect relationship between predator and prey is the fear of predator. When the prey gets the predator's signal (chemical/vocal), they will increase their vigilance time and reduce their foraging [7], such as mule deer v.s. mountain lions [8], elk v.s. wolves [9]. Consider the fear effect, Panday et al. [10] proposed the following model

$$\begin{cases} \frac{du}{dt} = \frac{R_0}{1+Kv}u\left(1-\frac{u}{K_0}\right) - \frac{CAuv}{B+u}, \\ \frac{dv}{dt} = \frac{Auv}{B+X} - Dv. \end{cases} \tag{1.1}$$

All parameters are positive. The biological interpretation of parameters is given in Table 1. They incorporated fear effect by modifying the prey intrinsic growth rate $R_0$ as $\frac{R_0}{1+Kv}$. By the scaling

$$\frac{u}{K_0} = \bar{u}, \quad \frac{Cv}{K_0} = \bar{v}, \quad R_0 t = \bar{t}, \quad \frac{AK_0}{R_0 B} = a, \quad \frac{K_0}{B} = b, \quad \frac{KK_0}{C} = c, \quad \frac{D}{R_0} = \mu, \tag{1.2}$$

model (1.1) is changed to (drop the bars)

$$\begin{cases} \frac{du}{dt} = \frac{u(1-u)}{1+cv} - \frac{auv}{1+bu}, \\ \frac{dv}{dt} = \frac{auv}{1+bu} - \mu v. \end{cases} \tag{1.3}$$

Panday et al. [10] introduced time delay of perceiving predator signals to model (1.3), and mainly studied the boundedness, persistence, local and global behavior of the delayed model.

**Table 1.** Biological description of parameters.

| Parameter | Definition | Parameter | Definition |
|---|---|---|---|
| $t$ | Time variable | $x$ | Spatial variable |
| $u$ | Prey density | $v$ | Predator density |
| $R_0$ | Prey intrinsic growth rate | $K_0$ | Prey carrying capacity |
| $A$ | Maximum predation rate | $B$ | Half-saturation constant of predator |
| $C^{-1}$ | Conversion efficiency | $D$ | Death rate of predators |
| $K$ | Fear parameter | $\tau$ | Averaged memory period of predator |
| $d_1$ | Diffusion coefficient of prey | $d_2$ | Diffusion coefficient of predator |
| $d$ | Memory-based diffusion coefficient | | |

In the real world, in addition to the fear effect of the prey, the clever predator also has spatial-memory and cognition [11], which is often ignored in modeling the predator-prey interaction. For example, blue whales rely on memory for migration, which is presented by B. Abrahms et al. [12] and W. F. Fagan [13]. As another example, animals in polar regions usually determine their spatial movement by judging footprints, which record the history of species distribution and movement, involving time delay [14]. Obviously, highly developed animals can even remember the historical distribution or cluster of species in space. Much progress has been made in implicitly integrating spatial cognition or memory [14–18]. To incorporate the memory effect, Shi et al. proposed a single specie model with spatial memory by introducing a additional delayed diffusion term [14]. They supposed that in addition to the negative gradient of the density distribution function at the present time, there is a directed movement toward the negative gradient of the density distribution function at past time [14]. After this pioneering work, some recent works [19–23] about the population model with memory effect have emerged. In [23], Song et al. obtained a computing method for the normal forms of the Hopf bifurcations in the diffusive predator-prey model with memory effect, which is friendly to use.

Inspired by the above work, we suppose the predator has spatial-memory diffusion and the prey has fear effect, then modified the model (1.3) as follow

$$\begin{cases} \dfrac{\partial u(x,t)}{\partial t} = d_1 \Delta u(x,t) + \dfrac{u(1-u)}{1+cv} - \dfrac{auv}{1+bu}, \\ \dfrac{\partial v(x,t)}{\partial t} = -d\nabla(v(x,t)\nabla u(x,t-\tau)) + d_2 \Delta v(x,t) + \dfrac{auv}{1+bu} - \mu v, \quad x \in \Omega,\ t > 0 \\ \dfrac{\partial u(x,t)}{\partial \bar{\nu}} = \dfrac{\partial v(x,t)}{\partial \bar{\nu}} = 0, \quad x \in \partial\Omega,\ t > 0 \\ u(x,\theta) = u_0(x,\theta) \geq 0, v(x,\theta) = v_0(x,\theta) \geq 0, \quad x \in \bar{\Omega}, \theta \in [-\tau, 0]. \end{cases} \tag{1.4}$$

All parameters are positive. The biological description of parameters is given in Table 1. The term $-d\nabla(v\nabla u(t-\tau))$ represents the memory-based diffusion effect of the predator. The Neumann boundary conditions is used. The aim of this paper is to study the effect of predator's memory-based diffusion and prey's fear on the model (1.4).

The rest of this paper is organized as follows. In Section 2, the stability of coexisting equilibrium and the existence of Hopf bifurcation are considered. In Section 3, the property of Hopf bifurcation is studied. In Section 3, some numerical simulations are given to analyze the effect of spatial-memory and fear effect. In Section 4, a short conclusion is given.

## 2. Stability analysis

For simplicity, we choose $\Omega = (0, l\pi)$. Denote $\mathbb{N}$ as positive integer set, and $\mathbb{N}_0$ as nonnegative integer set. It is easy to obtain $(0, 0)$ and $(1, 0)$ are two boundary equilibria of model (1.4). Next, we will give the existence of coexisting equilibrium.

**Lemma 2.1.** *If $a > (1 + b)\mu$, model* (1.4) *has one unique coexisting equilibrium $(u_*, v_*)$ where $u_* = \frac{\mu}{a-b\mu}$, $v_* = \frac{1}{2c}\left(-1 + \sqrt{1 + \frac{4c[a-(1+b)\mu]}{(a-b\mu)^2}}\right)$.*

*Proof.* The coexisting equilibrium of (1.4) is a positive root of the following equations

$$\begin{cases} \dfrac{u(1-u)}{1+cv} - \dfrac{auv}{1+bu} = 0, \\ \dfrac{auv}{1+bu} - \mu v = 0. \end{cases} \tag{2.1}$$

From the second equation, we have $u = \frac{\mu}{a-b\mu}$. Substitute it into the first equation, we have

$$cv^2 + v - \frac{(a-(1+b)\mu)}{(a-b\mu)^2} = 0.$$

Then $v = \frac{1}{2c}\left(-1 \pm \sqrt{1 + 4c\frac{(a-(1+b)\mu)}{(a-b\mu)^2}}\right)$. Obviously, the conclusion holds.

In this paper, we mainly study the stability of coexisting equilibrium $E_*(u_*, v_*)$. Linearize model (1.4) at $E_*(u_*, v_*)$, we have

$$\frac{\partial u}{\partial t}\begin{pmatrix} u(x,t) \\ u(x,t) \end{pmatrix} = D_1\begin{pmatrix} \Delta u(t) \\ \Delta v(t) \end{pmatrix} + D_2\begin{pmatrix} \Delta u(t-\tau) \\ \Delta v(t-\tau) \end{pmatrix} + L\begin{pmatrix} u(x,t) \\ v(x,t) \end{pmatrix}, \tag{2.2}$$

where

$$D_1 = \begin{pmatrix} d_1 & 0 \\ 0 & d_2 \end{pmatrix}, \quad D_2 = \begin{pmatrix} 0 & 0 \\ -dv_* & 0 \end{pmatrix}, \quad L = \begin{pmatrix} a_1 & a_2 \\ b_1 & 0 \end{pmatrix},$$

and $a_1 = u_*\left(\frac{abv_*}{(1+bu_*)^2} - \frac{1}{1+cv_*}\right)$, $a_2 = -\frac{u_*(1-u_*)(1+2cv_*)}{v_*(1+cv_*)^2} < 0$, $b_1 = \frac{av_*}{(1+bu_*)^2} > 0$. The characteristic equations are

$$\lambda^2 + A_n\lambda + B_n + C_n e^{-\lambda\tau} = 0, \quad n \in \mathbb{N}_0, \tag{2.3}$$

where

$$A_n = (d_1 + d_2)\frac{n^2}{l^2} - a_1, \quad B_n = -a_2b_1 - a_1d_2\frac{n^2}{l^2} + d_1d_2\frac{n^4}{l^4}, \quad C_n = -a_2dv_*\frac{n^2}{l^2}.$$

*2.1.* $\tau = 0$

When $\tau = 0$, the characteristic Eq (2.3) become

$$\lambda^2 + A_n\lambda + B_n + C_n = 0, \quad n \in \mathbb{N}_0, \tag{2.4}$$

where $B_n + C_n = -a_2b_1 - (a_2dv_* + a_1d_2)\frac{n^2}{l^2} + d_1d_2\frac{n^4}{l^4}$. Make the following hypothesis

$$(\mathbf{H_1}) \qquad a > (1+b)\mu, \;\; a_1 < 0.$$

**Theorem 2.1.** *For model* (1.4) *with* $\tau = 0$, $E_*(u_*, v_*)$ *is locally asymptotically stable under the hypothesis* $(\mathbf{H_1})$.

*Proof.* If $(\mathbf{H_1})$ holds, we can easily obtain that $A_n > 0$ and $B_n + C_n > 0$. Then the characteristic roots of (2.4) all have negative real parts. Then $E_*(u_*, v_*)$ is locally asymptotically stable.

*2.2.* $\tau > 0$

In the following, we assume $(\mathbf{H_1})$ holds. Let $\mathrm{i}\omega$ $(\omega > 0)$ be a solution of Eq (2.3), then we have

$$-\omega^2 + A_n\mathrm{i}\omega + B_n + C_n(\cos\omega\tau - \mathrm{i}\sin\omega\tau) = 0.$$

We can obtain $\cos\omega\tau = \frac{\omega^2 - B_n}{C_n}$, $\sin\omega\tau = \frac{A_n\omega}{C_n} > 0$ under hypothesis $(\mathbf{H_1})$. It leads to

$$\omega^4 + \left(A_n^2 - 2B_n\right)\omega^2 + B_n^2 - C_n^2 = 0. \tag{2.5}$$

Let $p = \omega^2$, then (2.5) becomes

$$p^2 + \left(A_n^2 - 2B_n\right)p + B_n^2 - C_n^2 = 0, \tag{2.6}$$

and the roots of (2.6) are $p_n^{\pm} = \frac{1}{2}[-\left(A_n^2 - 2B_n\right) \pm \sqrt{\left(A_n^2 - 2B_n\right)^2 - 4(B_n^2 - C_n^2)}]$. By direct computation, we have

$$\begin{cases} A_n^2 - 2B_n = a_1^2 + 2a_2b_1 - 2a_1d_1\dfrac{n^2}{l^2} + (d_1^2 + d_2^2)\dfrac{n^4}{l^4}, \\ B_n - C_n = d_1d_2\dfrac{n^4}{l^4} + (a_2dv_* - a_1d_2)\dfrac{n^2}{l^2} - a_2b_1, \end{cases}$$

and $B_n + C_n > 0$ under hypothesis $(\mathbf{H_1})$. Define $z_{\pm} = \frac{-(a_2dv_* - a_1d_2) \pm \sqrt{(a_2dv_* - a_1d_2)^2 - 4d_1d_2(-a_2b_1)}}{2d_1d_2}$, $d_* = \frac{a_1d_2}{a_2v_*} + \frac{2}{v_*}\sqrt{-\frac{b_1d_1d_2}{a_2}}$, and $\mathbb{M} = \{n | \frac{n^2}{l_2} \in (z_-, z_+),\ n \in \mathbb{N}_0\}$. Then we can obtain that

$$\begin{cases} B_n - C_n > 0, & \text{for } d \le d_*,\ n \in \mathbb{N}_0, \\ B_n - C_n > 0, & \text{for } d > d_*,\ n \notin \mathbb{M}, \\ B_n - C_n < 0, & \text{for } d > d_*,\ n \in \mathbb{M}. \end{cases} \tag{2.7}$$

The existence of purely imaginary roots of Eq (2.3) can be divided into the following two cases.

**Case 1** : $a_1^2 + 2a_2b_1 > 0$. We can obtain $A_n^2 - 2B_n > a_1^2 + 2a_2b_1 > 0$. For $d > d_*$ and $n \in \mathbb{M}$, Eq (2.3) has a pair of purely imaginary roots $\pm i\omega_n^+$ at $\tau_n^{j,+}$ for $j \in \mathbb{N}_0$ and $n \in \mathbb{M}$. Otherwise, Eq (2.3) does not have characteristic roots with zero real parts.

**Case 2** : $a_1^2 + 2a_2b_1 < 0$. This case can be divided into the following two subcases.

• For $d \le d_*$ and $n \in \mathbb{M}_1 := \{n | A_n^2 - 2B_n < 0,\ \left(A_n^2 - 2B_n\right)^2 - 4(B_n^2 - C_n^2) > 0,\ n \in \mathbb{N}_0\}$, Eq (2.3) has two pairs of purely imaginary roots $\pm i\omega_n^\pm$ at $\tau_n^{j,\pm}$ for $j \in \mathbb{N}_0$ and $n \in \mathbb{M}_1$. Otherwise, Eq (2.3) does not have characteristic roots with zero real parts.

• For $d > d_*$ and $n \in \mathbb{M}_2 := \{n | A_n^2 - 2B_n < 0,\ \left(A_n^2 - 2B_n\right)^2 - 4(B_n^2 - C_n^2) > 0,\ n \in \mathbb{N}_0,\ n \notin \mathbb{M}\}$, Eq (2.3) has two pairs of purely imaginary roots $\pm i\omega_n^\pm$ at $\tau_n^{j,\pm}$ for $j \in \mathbb{N}_0$ and $n \in \mathbb{M}_1$. For $d > d_*$ and $n \in \mathbb{M}$, Eq (2.3) has a pair of purely imaginary roots $\pm i\omega_n^+$ at $\tau_n^{j,+}$ for $j \in \mathbb{N}_0$ and $n \in \mathbb{M}$. Otherwise, Eq (2.3) does not have characteristic roots with zero real parts.

The $\omega_n^\pm$ and $\tau_n^{j,\pm}$ are defined as follow

$$\omega_n^\pm = \sqrt{p_n^\pm}, \quad \tau_n^{j,\pm} = \frac{1}{\omega_n^\pm}\arccos\left(\frac{(\omega_n^\pm)^2 - B_n}{C_n}\right) + 2j\pi. \tag{2.8}$$

Define

$$\mathbb{S} = \{\tau_n^{j,+} \text{ or } \tau_n^{j,-} | \text{Eq (2.3) has purely imaginary roots } \pm i\omega_n^+ \text{ or } \pm i\omega_n^- \text{ when } \tau = \tau_n^{j,+} \text{ or } \tau_n^{j,-}\}.$$

We have the following lemma.

**Lemma 2.2.** *Assume* ($\mathbf{H_1}$) *holds. Then* $Re(\frac{d\lambda}{d\tau})|_{\tau=\tau_n^{j,+}} > 0$, $Re(\frac{d\lambda}{d\tau})|_{\tau=\tau_n^{j,-}} < 0$ *for* $\tau_n^{j,\pm} \in \mathbb{S}$ *and* $j \in \mathbb{N}_0$.

*Proof.* By Eq (2.3), we have

$$\left(\frac{d\lambda}{d\tau}\right)^{-1} = \frac{2\lambda + A_n}{C_n\lambda e^{-\lambda\tau}} - \frac{\tau}{\lambda}.$$

Then

$$\begin{aligned}
\left[\mathrm{Re}\left(\frac{d\lambda}{d\tau}\right)^{-1}\right]_{\tau=\tau_n^{j,\pm}} &= \mathrm{Re}\left[\frac{2\lambda + A_n}{C_n\lambda e^{-\lambda\tau}} - \frac{\tau}{\lambda}\right]_{\tau=\tau_n^{j,\pm}} \\
&= \left[\frac{1}{A_n^2\omega^2 + (B_n - \omega)^2}(2\omega^2 + A_n^2 - 2B_n)\right]_{\tau=\tau_n^{j,\pm}} \\
&= \pm\left[\frac{1}{A_n^2\omega^2 + (B_n - \omega)^2}\sqrt{(A_n^2 - 2B_n)^2 - 4(B_n^2 - C_n^2)}\right]_{\tau=\tau_n^{j,\pm}}.
\end{aligned}$$

Therefore $\mathrm{Re}(\frac{d\lambda}{d\tau})|_{\tau=\tau_n^{j,+}} > 0$, $\mathrm{Re}(\frac{d\lambda}{d\tau})|_{\tau=\tau_n^{j,-}} < 0$.

Denote $\tau_* = min\{\tau_n^{0,\pm} |\ \tau_n^{0,\pm} \in \mathbb{S}\}$. We have the following theorem.

**Theorem 2.2.** *Assume* ($\mathbf{H_1}$) *holds, then the following statements are true for model* (1.4).

• $E_*(u_*, v_*)$ *is locally asymptotically stable for* $\tau > 0$ *when* $\mathbb{S} = \varnothing$.

• $E_*(u_*, v_*)$ *is locally asymptotically stable for* $\tau \in [0, \tau_*)$ *when* $\mathbb{S} \neq \varnothing$.

• $E_*(u_*, v_*)$ *is unstable for* $\tau \in (\tau_*, \tau_* + \varepsilon)$ *for some* $\varepsilon > 0$ *when* $\mathbb{S} \neq \varnothing$.

• *Hopf bifurcation occurs at* $(u_*, v_*)$ *when* $\tau = \tau_n^{j,+}$ $(\tau = \tau_n^{j,-})$, $j \in \mathbb{N}_0$, $\tau_n^{j,\pm} \in \mathbb{S}$.

**Remark 2.1.** *In the Theorem 2.2, if $E_*(u_*, v_*)$ is locally asymptotically stable, the densities of prey and predator will tend to the equilibrium state in the whole region when the initial densities of prey and predator is near $E_*(u_*, v_*)$. When Hopf bifurcation occurs at $(u_*, v_*)$, then the densities of prey and predator will produce periodic oscillation. Especially, spatially homogeneous periodic oscillations may occur when $\tau$ near the critical value $\tau = \tau_0^{j,+}$ or $\tau = \tau_0^{j,-}$, and spatially inhomogeneous periodic oscillations may occur when $\tau$ near the critical value $\tau = \tau_n^{j,+}$ or $\tau = \tau_n^{j,-}$ $(n > 0)$.*

## 3. Property of Hopf bifurcation

In this section, we use the algorithm in [23] to compute the normal form of Hopf bifurcation. We denote the critical value of Hopf bifurcation as $\tilde{\tau}$ and the purely imaginary roots as $\pm i\omega_n$ of Eq (2.3). Let $\bar{u}(x,t) = u(x,\tau t) - u_*$ and $\bar{v}(x,t) = v(x,\tau t) - v_*$. Drop the bar, the model (1.4) can be written as

$$\begin{cases} \dfrac{\partial u}{\partial t} = \tau[d_1\Delta u + \dfrac{(u+u_*)(1-(u+u_*))}{1+c(v+v_*)} - \dfrac{a(u+u_*)(v+v_*)}{1+b(u+u_*)}], \\ \dfrac{\partial v}{\partial t} = \tau[-d\nabla((v+v_*)\nabla(u(t-1)+u_*)) + d_2\Delta v + \dfrac{a(u+u_*)(v+v_*)}{1+b(u+u_*)} - \mu(v+v_*)]. \end{cases} \tag{3.1}$$

Define the real-valued Sobolev space $\mathbb{X} = \left\{U = (u,v)^T \in W^{2,2}(0,l\pi)^2,\ (\frac{\partial u}{\partial x}, \frac{\partial v}{\partial x})|_{x=0,l\pi} = 0\right\}$, the inner product

$$[U,V] = \int_0^{l\pi} U^T V dx, \quad \text{for } U,\ V \in \mathbb{X},$$

and $\mathbb{C} = C([-1,0];\mathbb{X})$. Set $\tau = \tilde{\tau} + \varepsilon$, where $\varepsilon$ is small perturbation. Then system (3.1) is rewritten as

$$\frac{dU(t)}{dt} = d(\varepsilon)\Delta(U_t) + L(\varepsilon)(U_t) + F(U_t,\varepsilon), \tag{3.2}$$

where for $\varphi = (\varphi,\varphi_2)^T \in \mathbb{C}$, $d(\varepsilon)\Delta$, $L(\varepsilon) : \mathbb{C} \to \mathbb{X}$, $F : \mathbb{C}\times\mathbb{R}^2 \to \mathbb{X}$. They are defined as

$$d(\varepsilon)\Delta(\varphi) = d_0\Delta(\varphi) + F^d(\varphi,\varepsilon),\ L(\varepsilon)(\varphi) = (\tilde{\tau}+\varepsilon)A\varphi(0),$$

$$F(\varphi,\varepsilon) = (\tilde{\tau}+\varepsilon)\begin{pmatrix} f(\phi^{(1)}(0)+u_*, \phi^{(2)}(0)+v_*) \\ g(\phi^{(1)}(0)+u_*, \phi^{(2)}(0)+v_*) \end{pmatrix} - L(\varepsilon)(\varphi),$$

and

$$d_0\Delta(\varphi) = \tilde{\tau}D_1\varphi_{xx}(0) + \tilde{\tau}D_2\varphi_{xx}(-1),$$

$$F^d(\varphi,\varepsilon) = -d(\tilde{\tau}+\varepsilon)\begin{pmatrix} 0 \\ \phi_x^{(1)}(-1)\phi_x^{(2)}(0) + \phi_{xx}^{(1)}(-1)\phi^{(2)}(0) \end{pmatrix} + \varepsilon\begin{pmatrix} d_1\phi_{xx}^{(1)}(0) \\ -dv_*\phi_{xx}^{(1)}(-1) + d_2\phi_{xx}^{(2)}(0) \end{pmatrix}.$$

Denote $L_0(\varphi) = \tilde{\tau}A\varphi(0)$, and rewrite (3.2) as

$$\frac{dU(t)}{dt} = d_0\Delta(U_t) + L_0(U_t) + \tilde{F}(U_t,\varepsilon), \tag{3.3}$$

where $\tilde{F}(\varphi,\varepsilon) = \varepsilon A\varphi(0) + F(\varphi,\varepsilon) + F^d(\varphi,\varepsilon)$. The characteristic equation for the linearized equation $\frac{dU(t)}{dt} = d_0\Delta(U_t) + L_0(U_t)$ is $\tilde{\Gamma}_n(\lambda) = det\left(\tilde{M}_n((\lambda))\right)$, where

$$\tilde{M}_n(\lambda) = \lambda I_2 + \tilde{\tau}\frac{n^2}{l^2}D_1 + \tilde{\tau}e^{-\lambda}\frac{n^2}{l^2}D_2 - \tilde{\tau}A. \tag{3.4}$$

The eigenvalue problem

$$-z(x)'' = \nu z(x), \quad x \in (0, l\pi); \quad z(0)' = z(l\pi)' = 0,$$

has eigenvalues $\frac{n^2}{l^2}$ and normalized eigenfunctions

$$z_n(x) = \frac{\cos\frac{nx}{l}}{\|\cos\frac{nx}{l}\|_{2,2}} = \begin{cases} \frac{1}{l\pi} & n = 0, \\ \frac{\sqrt{2}}{l\pi}\cos\frac{nx}{l} & n \neq 0, \end{cases} \tag{3.5}$$

Set $\beta_n^{(j)} = z_n(x)e_j$, $j = 1, 2$, where $e_1 = (1, 0)^T$ and $e_2 = (0, 1)^T$. Define $\eta_n(\theta) \in BV([-1, 0], \mathbb{R}^2)$, such that

$$\int_{-1}^{0} d\eta^n(\theta)\phi(\theta) = L_0^d(\varphi(\theta)) + L_0(\varphi(\theta)), \quad \varphi \in C,$$

$C = C([-1, 0], \mathbb{R}^2)$, $C^* = C([0, 1], \mathbb{R}^{2*})$, and

$$< \psi(s), \varphi(\theta) >= \psi(0)\varphi(0) - \int_{-1}^{0}\int_{0}^{\theta} \psi(\xi - \theta)d\eta^n(\theta)\varphi(\xi)d\xi, \quad \psi \in C^*, \ \varphi \in C. \tag{3.6}$$

Let $\bigwedge = \{i\tilde{\omega}, -i\tilde{\omega}\}$, the eigenspace $P$, and corresponding adjoint space $P^*$. Decompose $C = P \oplus Q$, where $Q = \{\varphi \in C :< \psi, \varphi >= 0, \forall\psi \in P^*\}$. Choose $\Phi(\theta) = (\phi(\theta), \bar{\phi}(\theta))$, $\Psi(\theta) = col(\psi^T(s), \bar{\psi}^T(s))$, where

$$\phi(\theta) = \phi e^{i\tilde{\omega}\theta} := \begin{pmatrix} \phi_1(\theta) \\ \phi_2(\theta) \end{pmatrix}, \quad \psi(s) = \psi e^{-i\tilde{\omega}s} := \begin{pmatrix} \psi_1(s) \\ \psi_2(s) \end{pmatrix},$$

$$\phi = \begin{pmatrix} 1 \\ \frac{1}{a_2}\left(-a_1 + d_1\frac{n^2}{l^2} + i\tilde{\omega}\right) \end{pmatrix}, \quad \psi = M\begin{pmatrix} 1 \\ \frac{a_2}{d_2\frac{n^2}{l^2} + i\tilde{\omega}} \end{pmatrix},$$

and

$$M = \left(-\frac{a_1l^2 - d_1n^2 - d_2n^2 - a_2dv_*e^{-i\tilde{\omega}}n^2\tilde{\tau} - 2il^2\tilde{\omega}}{d_2n^2 + il^2\tilde{\omega}}\right)^{-1}.$$

Then $\phi(\theta)$ and $\psi(s)$ are the bases of $P$ and $P^*$, respectively, and such that $< \phi, \psi >= I_2$.

By direct computation, we have

$$f_{20} = \begin{pmatrix} f_{20}^{(1)} \\ f_{20}^{(2)} \end{pmatrix}, \quad f_{11} = \begin{pmatrix} f_{11}^{(1)} \\ f_{11}^{(2)} \end{pmatrix}, \quad f_{02} = \begin{pmatrix} f_{02}^{(1)} \\ f_{02}^{(2)} \end{pmatrix},$$

$$f_{30} = \begin{pmatrix} f_{30}^{(1)} \\ f_{30}^{(2)} \end{pmatrix}, \quad f_{21} = \begin{pmatrix} f_{21}^{(1)} \\ f_{21}^{(2)} \end{pmatrix}, \quad f_{12} = \begin{pmatrix} f_{12}^{(1)} \\ f_{12}^{(2)} \end{pmatrix}, \quad f_{03} = \begin{pmatrix} f_{03}^{(1)} \\ f_{03}^{(2)} \end{pmatrix},$$

where $f_{20}^{(1)} = \frac{2abv_*}{(1+bu_*)^3} - \frac{2}{1+cv_*}$, $f_{11}^{(1)} = -\frac{a}{(1+bu_*)^2} + \frac{c(-1+2u_*)}{(1+cv_*)^2}$, $f_{02}^{(1)} = \frac{2c^2(1-u_*)u_*}{(1+cv_*)^3}$, $f_{30}^{(1)} = -\frac{6ab^2v_*}{(1+bu_*)^4}$, $f_{21}^{(1)} = \frac{2ab}{(1+bu_*)^3} + \frac{2c}{(1+cv_*)^2}$, $f_{12}^{(1)} = \frac{2c^2(1-2u_*)}{(1+cv_*)^3}$, $f_{03}^{(1)} = -\frac{6c^3(1-u_*)u_*}{(1+cv_*)^4}$, $f_{20}^{(2)} = -\frac{2abv_*}{(1+bu_*)^3}$, $f_{11}^{(2)} = \frac{a}{(1+bu_*)^2}$, $f_{02}^{(2)} = 0$, $f_{30}^{(2)} = \frac{6ab^2v_*}{(1+bu_*)^4}$, $f_{21}^{(2)} = -\frac{2ab}{(1+bu_*)^3}$, $f_{12}^{(2)} = 0$, $f_{03}^{(2)} = 0$. We can compute the following parameters

$$\begin{aligned} A_{20} &= f_{20}\phi_1(0)^2 + f_{02}\phi_2(0)^2 + 2f_{11}\phi_1(0)\phi_2(0) = \overline{A}_{02}, \\ A_{11} &= 2f_{20}\phi_1(0)\bar{\phi}_1(0) + 2f_{02}\phi_2(0)\bar{\phi}_2(0) + 2f_{11}(\phi_1(0)\bar{\phi}_2(0) + \bar{\phi}_1(0)\phi_2(0)), \\ A_{21} &= 3f_{30}\phi_1(0)^2\bar{\phi}_1(0) + 3f_{03}\phi_2(0)^2\bar{\phi}_2(0) + 3f_{21}\left(\phi_1(0)^2\bar{\phi}_2(0) + 2\phi_1(0)\bar{\phi}_1(0)\phi_2(0)\right) \\ &\quad + 3f_{12}\left(\phi_2(0)^2\bar{\phi}_1(0) + 2\phi_2(0)\bar{\phi}_2(0)\phi_1(0)\right), \end{aligned} \tag{3.7}$$

$$A_{20}^d = -2d\tau\begin{pmatrix} 0 \\ \phi_1(0)(-1)\phi_2(0)(0) \end{pmatrix} = \bar{A_{02}^d},\ \ A_{11}^d = -2d\tau\begin{pmatrix} 0 \\ 2\mathrm{Re}\,[\phi_1(-1)\bar{\phi}_2(0)] \end{pmatrix},$$

and $\widetilde{A}_{j_1j_2} = A_{j_1j_2} - 2\frac{n^2}{l^2}A^d_{j_1j_2}$ for $j_1, j_2 = 0, 1, 2,\ j_1 + j_2 = 2$. In addition, $h_{0,20}(\theta) = \frac{1}{l\pi}(\widetilde{M}_0(2i\tilde{\omega}))^{-1}A_{20}e^{2i\tilde{\omega}\theta}$, $h_{0,11}(\theta) = \frac{1}{l\pi}(\widetilde{M}_0(0))^{-1}A_{11}$, $h_{2n,20}(\theta) = \frac{1}{2l\pi}(\widetilde{M}_{2n}(2i\tilde{\omega}))^{-1}\widetilde{A}_{20}e^{2i\tilde{\omega}\theta}$, $h_{2n,11}(\theta) = \frac{1}{l\pi}(\widetilde{M}_{2n}(0))^{-1}\widetilde{A}_{11}$.

$$S_2(\phi(\theta), h_{n,q_1q_2}(\theta)) = 2\phi_1 h^{(1)}_{n,q_1q_2}f_{20} + 2\phi_2 h^{(2)}_{n,q_1q_2}f_{02} + 2(\phi_1 h^{(2)}_{n,q_1q_2} + \phi_2 h^{(1)}_{n,q_1q_2})f_{11},$$

$$S_2(\bar{\phi}(\theta), h_{n,q_1q_2}(\theta)) = 2\bar{\phi}_1 h^{(1)}_{n,q_1q_2}f_{20} + 2\bar{\phi}_2 h^{(2)}_{n,q_1q_2}f_{02} + 2(\bar{\phi}_1 h^{(2)}_{n,q_1q_2} + \bar{\phi}_2 h^{(1)}_{n,q_1q_2})f_{11},$$

$$S_2^{d,1}(\phi(\theta), h_{0,11}(\theta)) = -2d\tilde{\tau}\begin{pmatrix} 0 \\ \phi_1(-1)h^{(2)}_{0,11}(0) \end{pmatrix},\ \ S_2^{d,1}(\bar{\phi}(\theta), h_{0,11}(\theta)) = -2d\tilde{\tau}\begin{pmatrix} 0 \\ \bar{\phi}_1(-1)h^{(2)}_{0,20}(0) \end{pmatrix},$$

$$S_2^{d,1}(\phi(\theta), h_{2n,11}(\theta)) = -2d\tilde{\tau}\begin{pmatrix} 0 \\ \phi_1(-1)h^{(2)}_{2n,11}(0) \end{pmatrix},\ \ S_2^{d,1}(\bar{\phi}(\theta), h_{2n,20}(\theta)) = -2d\tilde{\tau}\begin{pmatrix} 0 \\ \bar{\phi}_1(-1)h^{(2)}_{2n,20}(0) \end{pmatrix},$$

$$S_2^{d,2}(\phi(\theta), h_{2n,11}(\theta)) = -2d\tilde{\tau}\begin{pmatrix} 0 \\ \phi_1(-1)h^{(2)}_{2n,11}(0) \end{pmatrix} - 2d\tilde{\tau}\begin{pmatrix} 0 \\ \phi_2(0)h^{(1)}_{2n,11}(-1) \end{pmatrix},$$

$$S_2^{d,2}(\bar{\phi}(\theta), h_{2n,20}(\theta)) = -2d\tilde{\tau}\begin{pmatrix} 0 \\ \bar{\phi}_1(-1)h^{(2)}_{2n,20}(0) \end{pmatrix} - 2d\tilde{\tau}\begin{pmatrix} 0 \\ \bar{\phi}_2(0)h^{(1)}_{2n,20}(-1) \end{pmatrix},$$

$$S_2^{d,3}(\phi(\theta), h_{2n,11}(\theta)) = -2d\tilde{\tau}\begin{pmatrix} 0 \\ \phi_2(0)h^{(1)}_{2n,11}(-1) \end{pmatrix},\ \ S_2^{d,3}(\bar{\phi}(\theta), h_{2n,20}(\theta)) = -2d\tilde{\tau}\begin{pmatrix} 0 \\ \bar{\phi}_1(0)h^{(2)}_{2n,20}(-1) \end{pmatrix}.$$

Then we have

$$\begin{aligned}
B_{21} =& \frac{3}{2l\pi}\psi^T A21,\\
B_{22} =& \frac{1}{l\pi}\psi^T(S_2(\phi(\theta), h_{0,11}(\theta)) + S_2(\bar{\phi}(\theta), h_{0,20}(\theta))) + \frac{1}{2l\pi}\psi^T(S_2(\phi(\theta), h_{2n,11}(\theta)) + S_2(\bar{\phi}(\theta), h_{2n,20}(\theta))),\\
B_{23} =& -\frac{1}{l\pi}\frac{n^2}{l^2}\psi^T(S_2^{d,1}(\phi(\theta), h_{0,11}(\theta)) + S_2^{d,1}(\bar{\phi}(\theta), h_{0,20}(\theta)))\\
&+ \frac{1}{2l\pi}\psi^T\sum_{j=1,2,3} b^{(j)}_{2n}(S_2^{d,j}(\phi(\theta), h_{2n,11}(\theta)) + S_2^{d,j}(\bar{\phi}(\theta), h_{2n,20}(\theta))),
\end{aligned}$$

where $b^{(1)}_{2n} = -\frac{n^2}{l^2}$, $b^{(2)}_{2n} = -2\frac{n^2}{l^2}$, $b^{(3)}_{2n} = -4\frac{n^2}{l^2}$. The normal form of the Hopf bifurcation is

$$\dot{z} = Bz + \frac{1}{2}\begin{pmatrix} B_1z_1\varepsilon \\ \bar{B}_1z_2\varepsilon \end{pmatrix} + \frac{1}{3!}\begin{pmatrix} B_2z_1^2z_2\varepsilon \\ \bar{B}_2z_1z_2^2\varepsilon \end{pmatrix} + O(|z|\varepsilon^2 + |z^4|), \tag{3.8}$$

where

$$B_1 = 2i\tilde{\omega}\psi^T\phi,\ \ B_2 = B_{21} + \frac{3}{2}(B_{22} + B_{23}).$$

By the coordinate transformation $z_1 = \omega_1 - i\omega_2$, $z_2 = \omega_1 + i\omega_2$, and $\omega_1 = \rho\cos\xi$, $\omega_2 = \rho\sin\xi$, the normal form (3.8) can be rewritten as

$$\dot{\rho} = K_1\varepsilon\rho + K_2\rho^3 + O(\rho\varepsilon^2 + |(\rho, \varepsilon)|^4), \tag{3.9}$$

where $K_1 = \frac{1}{2}\mathrm{Re}(B_1)$, $K_2 = \frac{1}{3!}\mathrm{Re}(B_2)$.

By the work [23], we have the following theorem.

**Theorem 3.1.** *If $K_1K_2 < 0 (> 0)$, the Hopf bifurcation is supercritical (subcritical), and the bifurcating periodic orbits is stable (unstable) for $K_2 < 0 (> 0)$.*

**Remark 3.1.** *In the Theorem 3.1, when Hopf bifurcation is supercritical (subcritical), then the bifurcating periodic solutions exist for $\tau > \tilde{\tau}$ ($\tau < \tilde{\tau}$), where $\tilde{\tau}$ is some critical value $\tau = \tau_n^{j,\pm}$. When the periodic solution is stable, the densities of prey and predator will produce periodic oscillation, and finally continue to oscillate.*

## 4. Numerical simulations

In this section, we give some numerical simulations to analyze the effect of spatial memory in predator and fear in prey on the model (1.4). Fix the following parameters

$$a = 0.5,\ b = 1,\ \mu = 0.2,\ d_1 = 0.1,\ d_2 = 0.2,\ l = 2. \tag{4.1}$$

### 4.1. The effect of d

If we choose $c = 1$, then model (1.4) has a unique coexisting equilibrium $(u_*, v_*) \approx (0.6667,\ 0.0.6667)$, and $a_1^2 + 2a_2b_1 \approx 0.0352 > 0$, $d_* \approx 0.6206$. To study the effect of memory-based diffusion coefficient $d$ on the model (1.4), we give the bifurcation diagram of model (1.4) with parameter $d$ as in Figure 1. By the Theorem 2.2, we know that $(u_*, v_*)$ is locally stable for $\tau \geq 0$ when $d < d_*$. But when $d > d_*$, the inhomogeneous Hopf bifurcation curves exist. This means that increasing parameter $d$ is not conducive to the stability of the equilibrium $(u_*, v_*)$, and the densities of prey and predator will produce spatially inhomogeneous periodic oscillation.

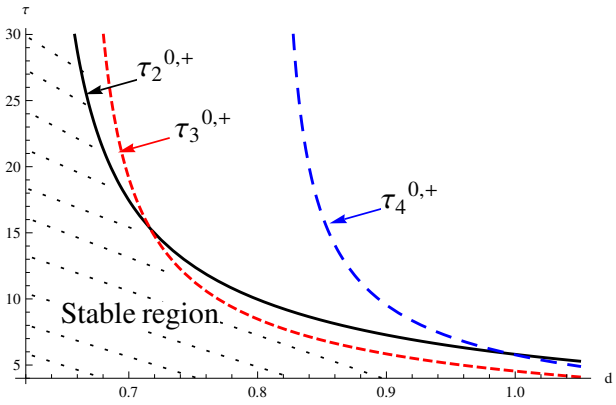


**Figure 1.** Stability region and Hopf bifurcation curves in $\tau - d$ plane. The dotted region is the stability region of $(u_*, v_*)$ and $\tau = \tau_i^{0,+}$, $i = 2, 3, 4$, are Hopf bifurcations curves.

### 4.2. The effect of τ

Choose $d = 0.7$, we have $\mathbb{M} = \{2,\ 3\}$ and $\tau_* = \tau_2^{0,+} \approx 17.4593 < \tau_3^{0,+} \approx 19.1380$. When $\tau \in [0, \tau_*)$, $(u_*, v_*)$ is locally stable (Figure 2). By direct calculation, we can obtain $K_1 \approx 0.0166$, and $K_2 \approx -0.0699$. Then, the Hopf bifurcation is supercritical and the bifurcating periodic solution is stable (Figure 3). At this time, the bifurcating periodic solution is spatially inhomogeneous and with mode-2.

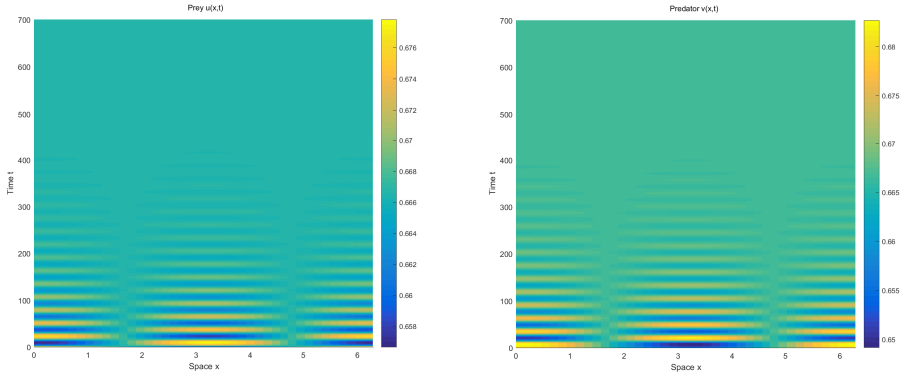


Prey $u(x,t)$ Predator $v(x,t)$

**Figure 2.** The numerical simulations of model (1.4) with $d = 0.7$, $\tau = 9$ and initial values $u_0(x) = u_* + 0.01\cos x$, $v_0(x) = v_* + 0.01\cos x$. The coexisting equilibrium $(u_*, v_*)$ is asymptotically stable.

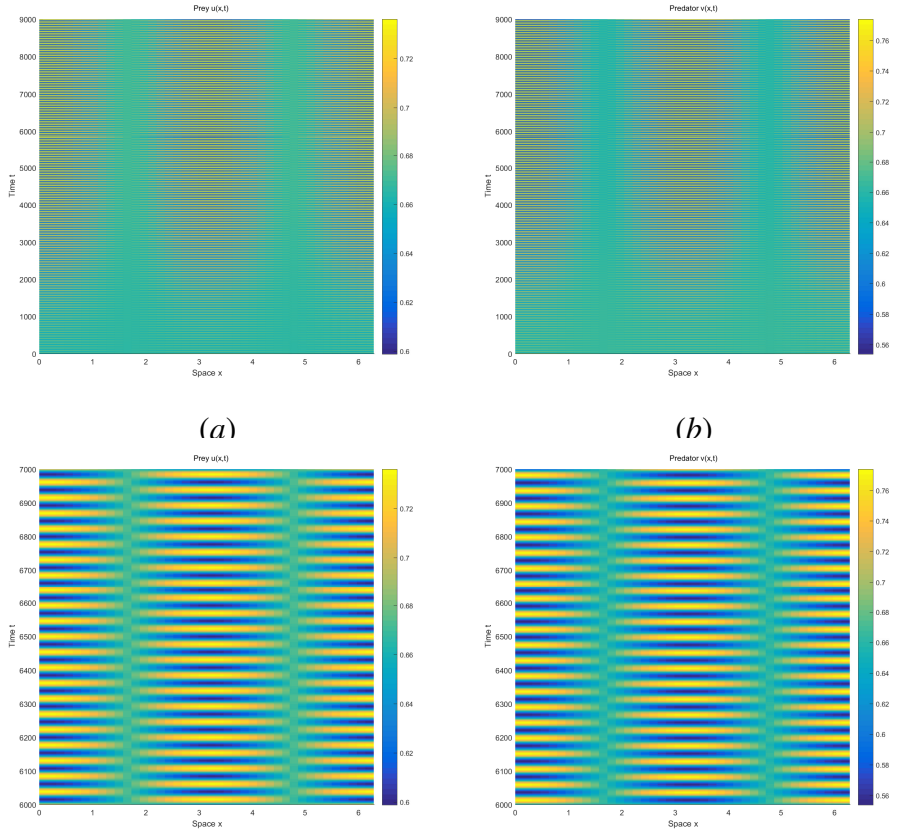


$(a)$ $(b)$

$(c)$ $(b)$

**Figure 3.** The numerical simulations of model (1.4) with $d = 0.7$, $\tau = 18$ and initial values $u_0(x) = u_* + 0.01\cos x$, $v_0(x) = v_* + 0.01\cos x$. The coexisting equilibrium $(u_*, v_*)$ is unstable and there exists a spatially inhomogeneous periodic solution with mode-2 spatial pattern.

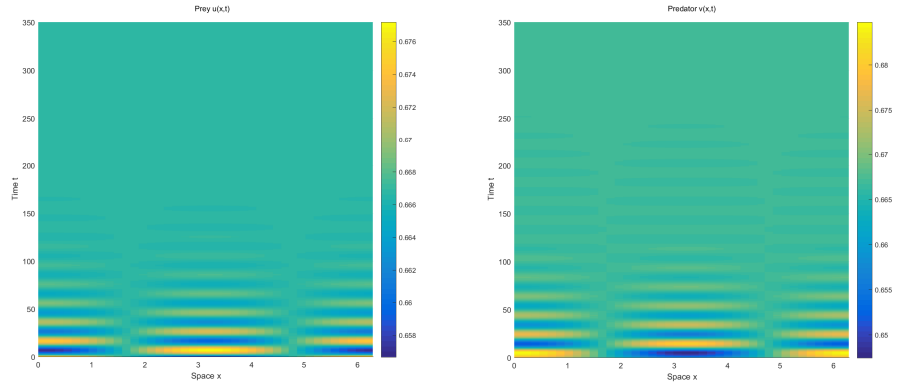


Prey $u(x,t)$ Predator $v(x,t)$

**Figure 4.** The numerical simulations of model (1.4) with $d = 0.8$, $\tau = 5$ and initial values $u_0(x) = u_* + 0.01\cos x$, $v_0(x) = v_* + 0.01\cos x$. The coexisting equilibrium $(u_*, v_*)$ is asymptotically stable.

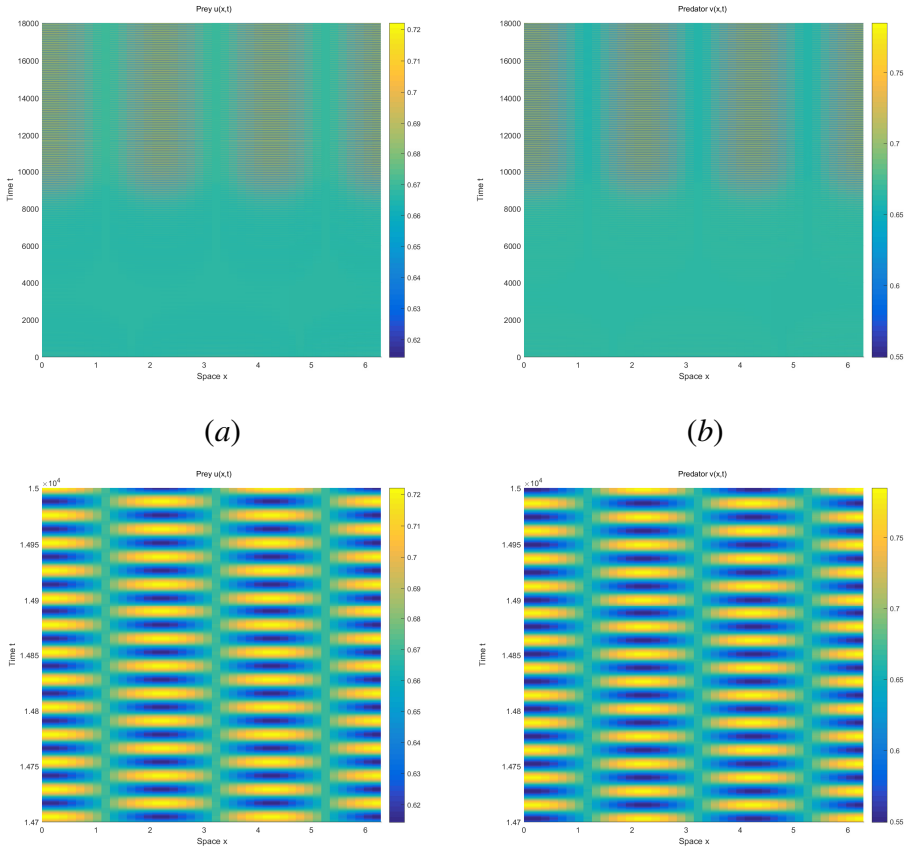


$(a)$ $(b)$

$(c)$ $(d)$

**Figure 5.** The numerical simulations of model (1.4) with $d = 0.8$, $\tau = 9$ and initial values $u_0(x) = u_* + 0.01\cos x$, $v_0(x) = v_* + 0.01\cos x$. The coexisting equilibrium $(u_*, v_*)$ is unstable and there exists a spatially inhomogeneous periodic solution with mode-3 spatial pattern.

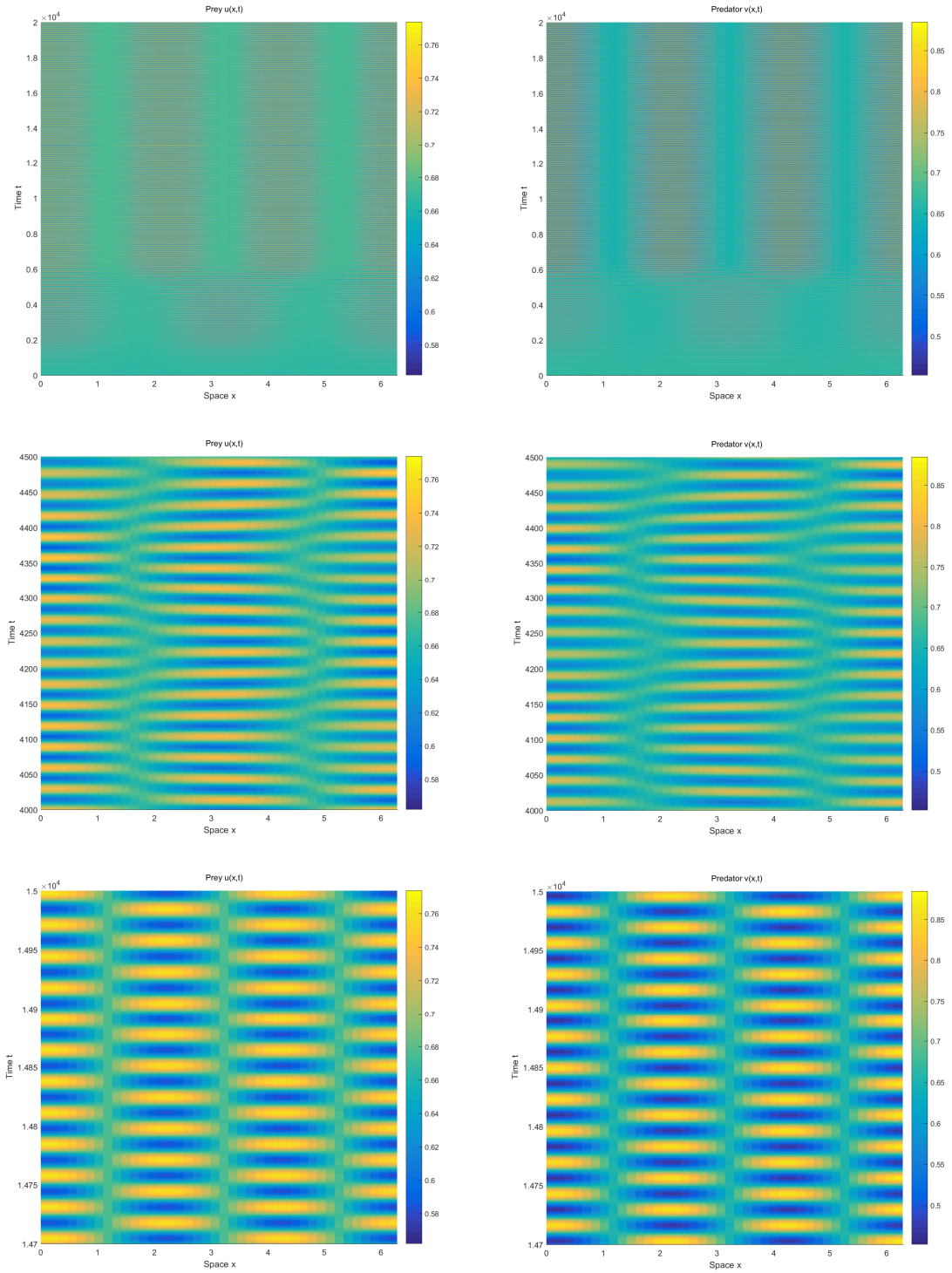


Prey $u(x,t)$ Predator $v(x,t)$

**Figure 6.** The numerical simulations of model (1.4) with $d = 0.8$, $\tau = 10$ and initial values $u_0(x) = u_* + 0.01\cos x$, $v_0(x) = v_* + 0.01\cos x$. The coexisting equilibrium $(u_*, v_*)$ is unstable and pattern transitions from a spatially inhomogeneous periodic solution with mode-2 to a spatially inhomogeneous periodic solution with mode-3.

Choose $d = 0.8$, we have $\mathbb{M} = \{2,\ 3\}$ and $\tau_* = \tau_3^{0,+} \approx 8.4754 < \tau_2^{0,+} \approx 9.9645$. When $\tau \in [0, \tau_*)$, $(u_*, v_*)$ is locally stable (Figure 4). By direct calculation, we can obtain $K_1 \approx 0.1236$, $K_2 \approx -0.3994$. Then, the Hopf bifurcation is supercritical and the bifurcating periodic solution is stable (Figure 5). At this time, the bifurcating periodic solution is spatially inhomogeneous with mode-3. When $\tau_* = \tau_3^{0,+} < \tau_2^{0,+} < \tau = 10$, there is an unstably spatially inhomogeneous periodic solution with mode-2 which transitions to the stably spatially inhomogeneous periodic solution with mode-3 (Figure 6).

### *4.3. The effect of c*

Next, we will study the effect of fear effect $c$ on the model (1.4). Fix the parameters as (4.1), then model (1.4) has a unique coexisting equilibrium $(u_*, v_*)$. And $a_1^2 + 2a_2b_1 > 0$ when $0 < c < 2.6194$. We give the figure of $d_*$ with parameter $c$ as in Figure 7. Set parameter $d = 0.7$ and $d = 0.8$, we give the bifurcation diagrams of model (1.4) with parameter $c$ as in Figure 8.

When $d = 0.7$ and $\tau = 20$, increasing parameter $c$ can destroy the stability of the coexisting equilibrium $(u_*, v_*)$, and induce spatially inhomogeneous periodic solution (Figure 9). This means that increasing parameter $c$ is not conducive to the stability of the coexisting equilibrium $(u_*, v_*)$.

When $d = 0.8$ and $\tau = 9$, increasing parameter $c$ can destroy the stability of the coexisting equilibrium $(u_*, v_*)$, and induce spatially inhomogeneous periodic solution initially (Figure 10). But when $c$ is larger enough, increasing parameter $c$ can rule out the spatially inhomogeneous periodic oscillation and stabilize the coexisting equilibrium $(u_*, v_*)$ (Figure 10). This means that increasing parameter $c$ is not conducive to the stability of the equilibrium $(u_*, v_*)$, initially. But when $c$ is large, increasing parameter $c$ is conducive to the stability of the coexisting equilibrium $(u_*, v_*)$.

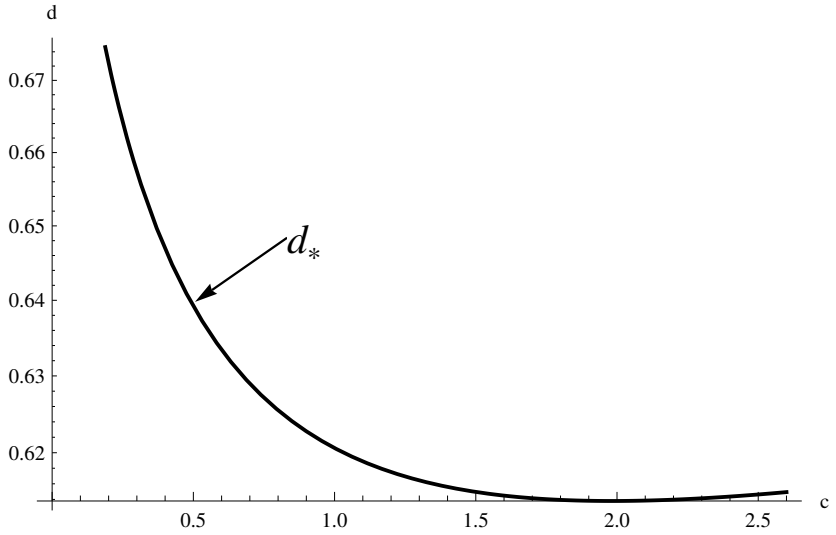


**Figure 7.** Figure of $d_*$ with parameter $c$.

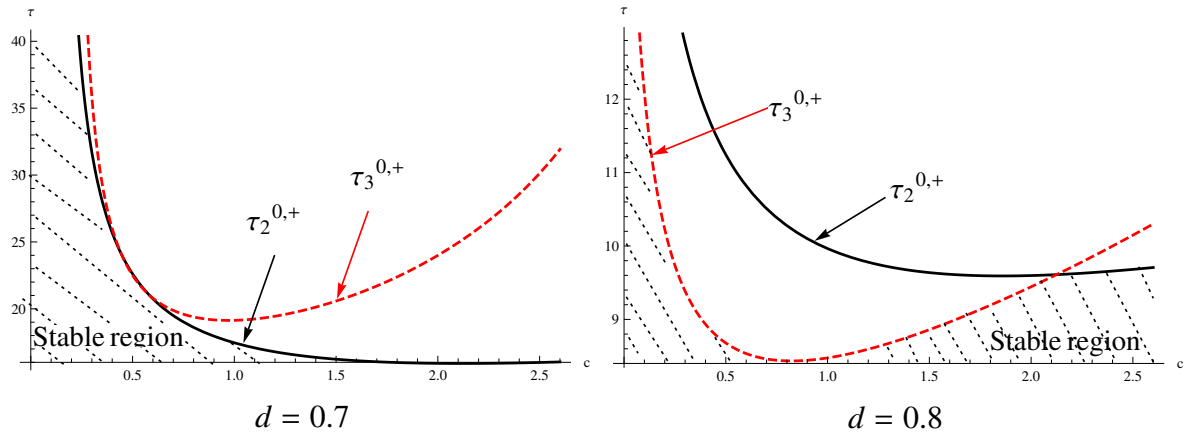


**Figure 8.** Stability region and Hopf bifurcation curves in $\tau - c$ plane. The dotted region is the stability region of $(u_*, v_*)$ and $\tau = \tau_i^{0,+}$, $i = 2, 3$, are Hopf bifurcations curves.

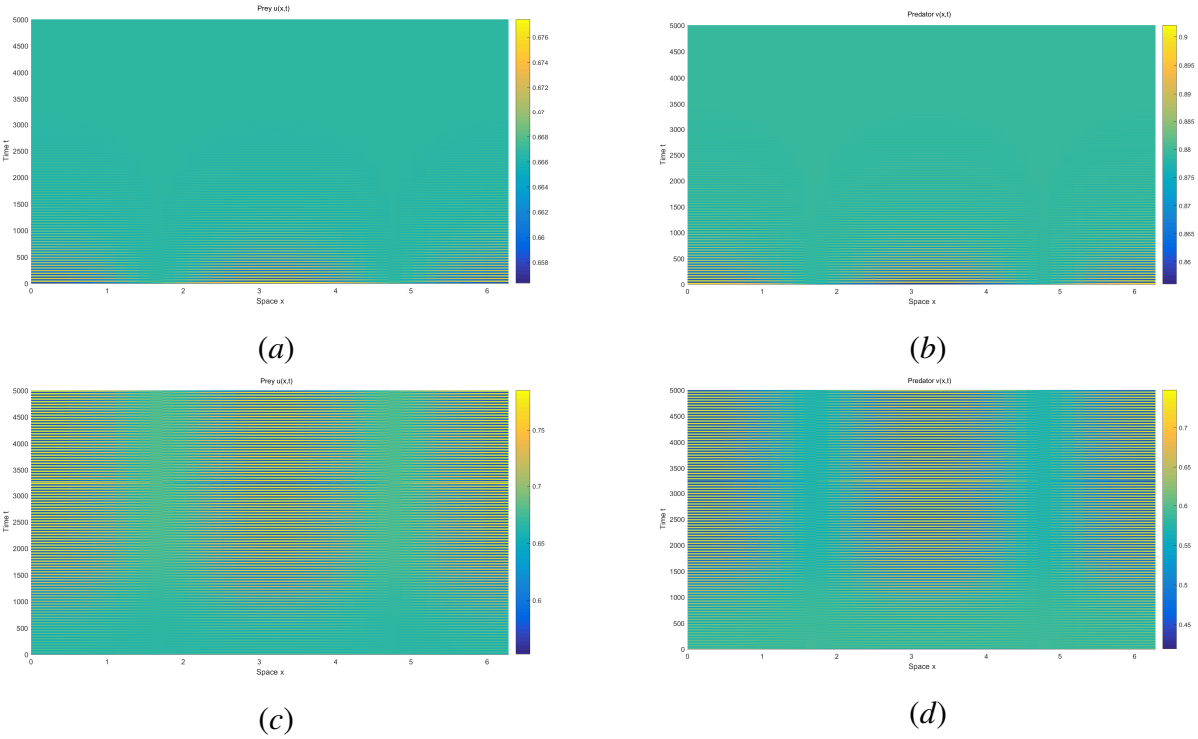


**Figure 9.** The numerical simulations of model (1.4) with $d = 0.7$, $\tau = 20$ and initial values $u_0(x) = u_* + 0.01\cos x$, $v_0(x) = v_* + 0.01\cos x$. The coexisting equilibrium $(u_*, v_*)$ is asymptotically stable for $c = 0.3$ ($(a)$, $(b)$). The coexisting equilibrium $(u_*, v_*)$ is unstable and there exists a spatially inhomogeneous periodic solution with mode-2 for $c = 1.5$ ($(c)$, $(d)$).

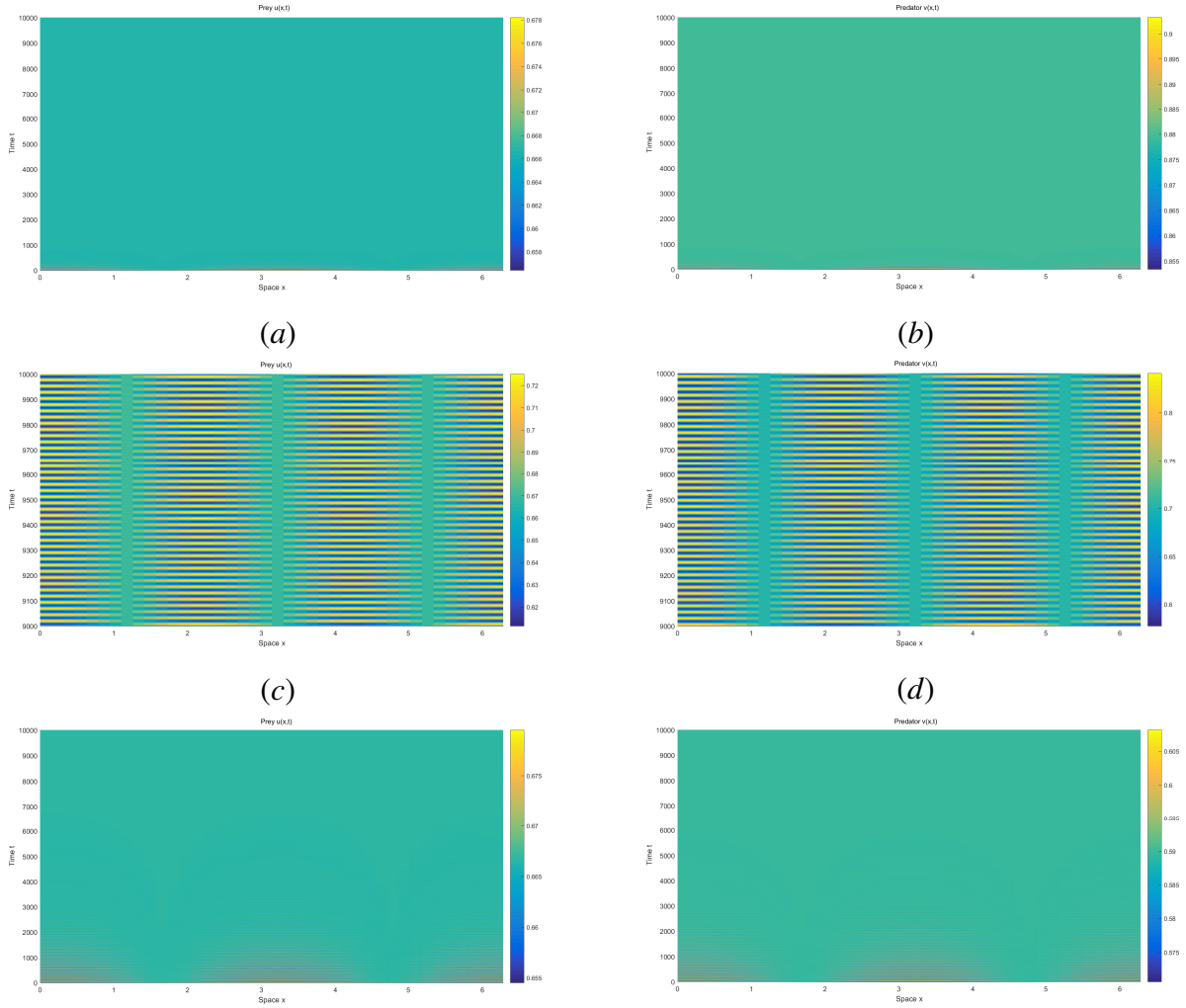


**Figure 10.** The numerical simulations of model (1.4) with $d = 0.8$, $\tau = 9$ and initial values $u_0(x) = u_* + 0.01\cos x$, $v_0(x) = v_* + 0.01\cos x$. The coexisting equilibrium $(u_*, v_*)$ is asymptotically stable for $c = 0.3$ ($(a)$, $(b)$) and $c = 1.5$ ($(e)$, $(f)$). The coexisting equilibrium $(u_*, v_*)$ is unstable and there exists a spatially inhomogeneous periodic solution with mode-3 for $c = 0.8$ ($(c)$, $(d)$).

## 5. Conclusions

In this paper, we incorporate the memory effect in predator and fear effect in prey into a predator-prey model. By using time delay in the memory of predator as bifurcating parameter, we analyze the local stability of coexisting equilibrium, the existence of Hopf bifurcation, and the property of Hopf bifurcation by the method in [23]. Through the numerical simulations, we analyzed the effect of memory effect in predator and fear in prey on the model.

The spatial memory effect plays an important role in the dynamics of the predator-prey model. Through the numerical simulations, we observed that the memory-based diffusion coefficient $d$ has

destabilizing effect on the predator-prey model when it is larger than some critical value. In addition. when $d$ crosses the critical value, time delay $\tau$ in the memory of predator can affect the stability of the equilibrium $(u_*, v_*)$. In the numerical simulations, we observe that the first Hopf bifurcation curve is inhomogeneous bifurcation curve, and homogeneous Hopf bifurcation curve does not exist. This is different from the predator-prey model without the spatial memory effect. When $\tau$ crosses the critical value $\tau_*$, the densities of prey and predator will produce spatially inhomogeneous periodic oscillation. When $\tau$ crosses the second critical value, the spatially inhomogeneous periodic oscillations with different modes exist, but the densities of prey and predator will converge to the spatially inhomogeneous periodic solution corresponding to the first bifurcation curve. This shows that the spatially memory effect in predator can destroy the stability of the coexisting equilibrium, and induce spatially inhomogeneous periodic oscillations.

In addition, the fear effect parameter $c$ in prey can also affect the stability of the coexisting equilibrium $(u_*, v_*)$. A small fear effect parameter $c$ means a large birth rate $\frac{1}{1+cv}$, then the large birth rate can support fluctuations. Increasing parameter $c$ can destroy the stability of the coexisting equilibrium $(u_*, v_*)$, and induce spatially inhomogeneous periodic solution. Hence, we observed the destabilizing effect on the the coexisting equilibrium $(u_*, v_*)$. A large fear effect parameter $c$ means a low birth rate, then the low birth rate can not support fluctuations. Increasing parameter $c$ can rule out the spatially inhomogeneous periodic oscillation and stabilize the coexisting equilibrium $(u_*, v_*)$. Hence, we observed the stabilizing effect on the the coexisting equilibrium $(u_*, v_*)$.

## Acknowledgements

This research is supported by the Fundamental Research Funds for the Central Universities (Grant No. 2572022BC01) and Postdoctoral Program of Heilongjiang Province (No. LBH-Q21060).

## Conflict of interest

The authors have no relevant financial or non-financial interests to disclose.

## References

1. R. Yang, C. Zhang, Dynamics in a diffusive predator-prey system with a constant prey refuge and delay, *Nonlinear Anal. Real World Appl.*, **31** (2016), 1–22. https://doi.org/10.1016/j.nonrwa.2016.01.005
2. R. Yang, Q. Song, Y. An, Spatiotemporal dynamics in a predator-prey model with functional response increasing in both predator and prey densities, *Mathematics*, **10** (2022), 17. https://doi.org/10.11948/20190295
3. Y. Liu, D. Duan, B. Niu, Spatiotemporal dynamics in a diffusive predator-prey model with group defense and nonlocal competition, *Appl. Math. Lett.*, **103** (2020), 106175. https://doi.org/10.1016/j.aml.2019.106175
4. R. Yang, L. Wang, D. Jin, Hopf bifurcation analysis of a diffusive nutrient-phytoplankton model with time delay, *Axioms*, **11** (2020), 56. https://doi.org/10.3390/axioms11020056

5. D. Geng, W. Jiang, Y. Lou, H. Wang, Spatiotemporal patterns in a diffusive predator-prey system with nonlocal intraspecific prey competition, *Stud. Appl. Math.*, **148** (2022), 396–432. https://doi.org/10.1111/sapm.12444
6. R. Yang, X. Zhao, Y. An, Dynamical analysis of a delayed diffusive predator-prey model with additional food provided and anti-predator behavior, *Mathematics*, **10** (2022), 469. https://doi.org/10.3390/math10030469
7. S. Lima, L. Dill, Behavioral decisions made under the risk of predation: a review and prospectus, *Can. J. Zool.*, **68** (1990), 619–640. https://doi.org/10.1139/z90-092
8. K. B. Altendorf, J. W. Laundré, C. A. L. González, J. S. Brown, Assessing effects of predation risk on foraging behavior of mule deer, *J. Mammal.*, **82** (2001), 430–439. https://doi.org/10.1644/1545-1542(2001)082¡0430:AEOPRO¿2.0.CO;2
9. S. Creel, D. Christianson, S. Liley, J. A. Winnie, Predation risk affects reproductive physiology and demography of elk, *Science*, **315** (2007), 960. https://doi.org/10.1126/science.1135918
10. P. Panday, S. Samanta, N. Pal, J. Chattopadhyay, Delay induced multiple stability switch and chaos in a predator-prey model with fear effect, *Math. Comput. Simul.*, **172** (2019), 134–158. https://doi.org/10.1016/j.matcom.2019.12.015
11. W. F. Fagan, M. A. Lewis, M. Auger-Méthé, T. Avgar, S. Benhamou, G. Breed, et al., Spatial memory and animal movement, *Ecol. Lett.*, **16** (2014), 1316–1329. https://doi.org/10.1111/ele.12165
12. B. Abrahms, E. L. Hazen, E. O. Aikens, M. S. Savoca, J. A. Goldbogen, S. J. Bograd, et al., Memory and resource tracking drive blue whale migrations, *Proc. Natl. Acad. Sci.*, **116** (2019), 5582–5587. https://doi.org/10.1073/pnas.1819031116
13. W. F. Fagan, Migrating whales depend on memory to exploit reliable resources, *Proc. Natl. Acad. Sci.*, **116** (2019), 5217–5219. https://doi.org/10.1073/pnas.1901803116
14. J. Shi, C. Wang, H. Wang, X. Yan, Diffusive spatial movement with memory, *J. Dyn. Differ. Equations*, **32** (2020), 979–1002. https://doi.org/10.1007/s10884-019-09757-y
15. P. R. Moorcroft, M. A. Lewis, R. L. Crabtree, Home range analysis using amechanistic home range model, *Ecology*, **80** (1999), 1656–1665. https://doi.org/10.1890/0012-9658(1999)080[1656:HRAUAM]2.0.CO;2
16. M. A. Lewis, J. D. Murray, Modelling territoriality and wolf-deer interactions, *Nature*, **366** (1993), 738–740. https://doi.org/10.1038/366738a0
17. J. R. Potts, M. A. Lewis, Spatial memory and taxis-driven pattern formation in model ecosystems, *Bull. Math. Biol.*, **81** (2019), 2725–2747. https://doi.org/10.1007/s11538-019-00626-9
18. J. R. Potts, M. A. Lewis, How memory of direct animal interactions can lead to territorial pattern formation, *J. R. Soc. Interface*, **13** (2016), 20160059. https://doi.org/10.1098/rsif.2016.0059
19. Q. An, C. Wang, H. Wang, Analysis of a spatial memory model with nonlocal maturation delay and hostile boundary condition, *Discrete Contin. Dyn. Syst.*, **40** (2020), 5845–5868. https://doi.org/10.3934/dcds.2020249
20. J. Shi, C. Wang, H. Wang, Diffusive spatial movement with memory and maturation delays, *Nonlinearity*, **32** (2019), 3188–3208. https://doi.org/10.1088/1361-6544/ab1f2f

21. Q. Shi, J. Shi, H. Wang, Spatial movement with distributed memory, *J. Math. Biol.*, **82** (2021), 33. https://doi.org/10.1007/s00285-021-01588-0

22. Y. Song, S. Wu, H. Wang, Spatiotemporal dynamics in the single population model with memory-based diffusion and nonlocal effect, *J. Differ. Equations*, **267** (2019), 6316–6351. https://doi.org/10.1016/j.jde.2019.06.025

23. Y. Song, Y. Peng, T. Zhang, The spatially inhomogeneous Hopf bifurcation induced by memory delay in a memory-based diffusion system, *J. Differ. Equations*, **300** (2021), 597–624. https://doi.org/10.1016/j.jde.2021.08.010


AIMS Press